Available online at www.sciencedirect.com
ScienceDirect
Journal of Molecular Catalysis A: Chemical 261 (2007) 79–87
JOURNAL OF MOLECULAR CATALYSIS A: CHEMICAL
www.elsevier.com/locate/molcata

New chloro and triphenylsiloxy derivatives of dioxomolybdenum(VI) chelated with pyrazolylpyridine ligands: Catalytic applications in olefin epoxidation

Sofia M. Bruno [a], Cláudia C.L. Pereira [a], Maria Salete Balula [a], Mariela Nolasco [a], Anabela A. Valente [a,*], Alan Hazell [b], Martyn Pillinger [a], Paulo Ribeiro-Claro [a], Isabel S. Gonçalves [a,**]

[a] *Department of Chemistry, CICECO, University of Aveiro, Campus de Santiago, 3810-193 Aveiro, Portugal*
[b] *Department of Chemistry, University of Aarhus, Langelandsgade 140, DK-8000 Aarhus C, Denmark*

Received 30 June 2006; received in revised form 21 July 2006; accepted 24 July 2006
Available online 7 September 2006

Abstract

Dioxomolybdenum(VI) complexes of general formula $[MoO_2X_2L_2]$ (X = Cl, $OSiPh_3$; L_2 = 2-(1-butyl-3-pyrazolyl)pyridine, ethyl[3-(2-pyridyl)-1-pyrazolyl]acetate) were prepared and characterised by ^{1}H NMR, IR and Raman spectroscopy. The assignment of the vibrational spectra was supported by ab initio calculations. A single crystal X-ray diffraction study of the complex $[MoO_2Cl_2\{$ethyl[3-(2-pyridyl)-1-pyrazolyl]acetate$\}]$ showed that the compound is monomeric and crystallises in the tetragonal system with space group $P4_1$. The four complexes are active and selective catalysts for the liquid-phase epoxidation of olefins by *tert*-butylhydroperoxide. Selectivities to the corresponding epoxides were mostly 100% (for conversions of at least 34%) for the substrates cyclooctene, cyclododecene, 1-octene, *trans*-2-octene and (*R*)-(+)-limonene. For styrene epoxidation, the corresponding diol was also formed in significant quantities. The turnover frequencies for cyclooctene epoxidation at 55 °C were around 340 mol mol_{Mo}^{-1} h^{-1} for the chloro complexes and 160 mol mol_{Mo}^{-1} h^{-1} for the triphenylsiloxy complexes. The addition of co-solvents (1,2-dichloroethane or *n*-hexane) had a detrimental effect on catalytic activities. Kinetic studies for the two complexes bearing the ligand ethyl[3-(2-pyridyl)-1-pyrazolyl]acetate revealed an apparent first order dependence of the initial rate of cyclooctene conversion with respect to cyclooctene or oxidant concentration.

Keywords: Epoxidation; Homogeneous catalysis; Molybdenum; Pyrazolylpyridine ligands; Dioxomolybdenum(VI) complexes

1. Introduction

High oxidation state molybdenum oxo compounds are dominated by monooxo and *cis*-dioxomolybdenum species. Over the last 20 years or so, several tetracoordinate dioxomolybdenum(VI) complexes of the formula $[MoO_2(OR)_2]$ (R = Me, Et, *n*-Pr, Ph [1], *t*-Bu, *i*-Pr, CH_2*t*-Bu [2], 2,6-di-*tert*-butylphenyl [3]) and $[MoO_2(OSiR_3)_2]$ (R = *t*-Bu [4], Ot-Bu [5], Ph [6]) have been reported. Of these, the only structurally characterised examples are the diaryloxide MoO_2(O-2,6-*t*-$Bu_2C_6H_3)_2$·HO-2,6-*t*-$Bu_2C_6H_3$ [3] and the triphenylsiloxy complex, $[MoO_2(OSiPh_3)_2]$ [6]. The molecular structures of these two compounds show distorted tetrahedral coordination geometries. The tetrahedral structure is also known for the MoO_4^{2-} ion, and $[MoO_2X_2]$ (X = halide) is tetrahedral in the gas phase. Treatment of $[MoO_2X_2]$ species (X = halide, OR, $OSiR_3$) with Lewis bases, such as pyridine, 2,2′-bipyridine and 1,10-phenanthroline, and with donor solvents, such as acetonitrile and THF, gives adducts of the composition $[MoO_2X_2L_2]$ [1,2,7–18], which are generally more amenable to single crystal X-ray diffraction studies. The first crystal structure of a $[MoO_2X_2L_2]$-type complex was reported in 1968 (X = Cl and L = DMF) [19]. These species always present a distorted octahedral geometry [20], with the oxo ligands cis to each other in order to maximise the back-donation into the empty t_{2g} set orbitals. Most often, the arrangement of the anionic X and neutral L ligands are trans and cis, respectively [21].

* Corresponding author.
** Corresponding author. Tel.: +351 234370084.
E-mail address: igoncalves@dq.ua.pt (I.S. Gonçalves).

1381-1169/$ – see front matter © 2006 Elsevier B.V. All rights reserved.
doi:10.1016/j.molcata.2006.07.064

The $[MoO_2X_2L_2]$-type complexes are of interest as molydoenzyme models, oxo-transfer reagents, and catalysts for the epoxidation of olefins. The siloxyligated MoO_2^{2+} complexes, $[MoO_2(OSiR_3)_2L_2]$, also serve as models for isolated molybdenum atoms on a silica surface. For example, covalently anchored species of the type $MoO_2[(–O)_3SiO]Cl(THF)_n$ were previously characterised by EXAFS for a mesoporous silica grafted with the complex $[MoO_2Cl_2(THF)_2]$ [22]. The complex $[MoO_2(OSiPh_3)_2bpy]$ (bpy = 2,2′-bipyridine) exhibits good selectivity but a low turnover frequency (TOF) of about 12 mol mol_{Mo}^{-1} h^{-1} for the catalytic epoxidation of cyclooctene in liquid-phase, using *tert*-butylhydroperoxide (*t*-BuOOH) as the oxidant and a reaction temperature of 55 °C [9]. This is not very surprising since the corresponding $[MoO_2X_2L_2]$-type complexes (X = halide) with the polypyridyl ligands bpy and 2,2′-bipyrimidine are also rather slow catalysts of generally low activity [17]. On the other hand, we have recently shown that other ligands such as substituted 1,4-diazabutadienes and pyrazolylpyridines are more promising as supporting ligands [23,24], giving initial specific reaction rates as high as 360 mol mol_{Mo}^{-1} h^{-1} in the case of the complex $[MoO_2Cl_2$\{ethyl[3-(2-pyridyl)-1-pyrazolyl]acetate\}]. It is thought that the variable catalytic activities observed for $[MoO_2X_2L_2]$-type complexes and also molybdenum oxodiperoxo complexes $[MoO(O_2)_2L_2]$ are due, at least in part, to differences in the Lewis acidity of the metal centre as a result of the different donor properties of the ligands [25].

The high potential of substituted pyrazolylpyridines as supporting ligands for oxomolybdenum catalysts has already been well established for oxodiperoxo complexes of the type $[MoO(O_2)_2L]$ [25–28]. Herein, the preparation of $[MoO_2X_2L_2]$-type (X = Cl, $OSiPh_3$) complexes bearing substituted pyrazolylpyridines is described, and we report on their catalytic activity and kinetics in cyclooctene epoxidation using *t*-BuOOH as the oxidant. One aim of the present work is to examine how the catalytic behaviour is influenced by changing the nature of X from Cl to $OSiPh_3$ in an otherwise identical molecule. The crystal structure of the complex $[MoO_2Cl_2$\{ethyl[3-(2-pyridyl)-1-pyrazolyl]acetate\}] is also described.

2. Experimental

2.1. Materials and methods

Microanalyses were performed at University of Aveiro. ^{1}H NMR spectra were obtained using a Bruker CXP 300 spectrometer. Room-temperature FT-IR spectra were recorded with a Mattson 7000 FT-IR spectrometer, using a globar source, a deuterated triglycine sulphate (DTGS) detector, and potassium bromide cells, with 2 cm^{-1} resolution and triangular apodisation. The room temperature FT-Raman spectra were recorded on a RFS-100 Bruker FT-spectrometer, using a Nd:YAG laser (Coherent Compass-1064/500) with an excitation wavelength of 1064 nm and 2 cm^{-1} resolution.

All preparations and manipulations were carried out using standard Schlenk techniques under nitrogen. Solvents were dried by standard procedures (diethyl ether, *n*-hexane and THF with Na/benzophenone ketyl; acetonitrile and 1,2-dichloroethane with CaH_2), distilled under nitrogen and kept over 3 Å (for acetonitrile) or 4 Å molecular sieves. Silver molybdate (Ag_2MoO_4) was synthesised from silver nitrate (José M. Vaz Pereira) and sodium molybdate (Merck), and dried in vacuum at 60 °C for several hours prior to use. Triphenylchlorosilane and acetone-d_6 were purchased from Aldrich and used as received. Literature procedures were used to prepare $[MoO_2Cl_2(THF)_2]$ [29], $[MoO_2(OSiPh_3)_2]$ [6], ethyl[3-(2-pyridyl)-1-pyrazolyl]acetate [26], 2-(1-butyl-3-pyrazolyl)pyridine [26] and $[MoO_2Cl_2$\{ethyl[3-(2-pyridyl)-1-pyrazolyl]acetate\}] (**1**) [24].

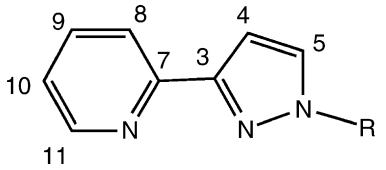

Plate 1. Numbering scheme for the assignment of the NMR spectra of complexes **2**–**4**.

2.2. *[MoO_2Cl_2[2-(1-butyl-3-pyrazolyl)pyridine]] (**2**)*

$[MoO_2Cl_2]$ (0.20 g, 1.00 mmol) was dissolved in THF (20 mL) and the solution was stirred for 20 min at 50 °C. An excess of 2-(1-butyl-3-pyrazolyl)pyridine (0.30 g, 1.50 mmol) was added, and the mixture stirred for 3 h. The resultant dark pink precipitate was filtered, washed with diethyl ether (3 × 15 mL) and dried under reduced pressure (0.37 g, 93%). Anal. Calcd. for $C_{12}H_{15}N_3Cl_2MoO_2$ (400.11): C, 36.02; H, 3.77; N, 10.50. Found: C, 36.27; H, 4.16; N, 9.90. Selected IR (KBr): 3142m, 2959m, 2936m, 2862m, 1612s, 1569m, 1535w, 1505m, 1466s, 1442s, 1432m, 1368s, 1341m, 1236s, 1081s, 937s, 908vs, 780vs, 345m cm^{-1}. ^{1}H NMR (300.13 MHz, 25 °C, acetone-d_6): δ = 9.22 ppm (d, 1H, H^{11}), 8.19–8.11 ppm (c, 3H, H^9, H^8, H^5), 7.68 ppm (dt, 1H, H^{10}), 7.18 ppm (d, 1H, H^4), 4.74 ppm (*t*, 2H, N–CH_2), 2.01–1.91 ppm (m, 2H, CH_2), 1.27–1.20 ppm (m, 2H, CH_2), 0.79 ppm (t, 3H, CH_3) (Plate 1).

2.3. *[$MoO_2(OSiPh_3)_2$\{ethyl[3-(2-pyridyl)-1-pyrazolyl]acetate\}] (**3**)*

A suspension of Ag_2MoO_4 (0.38 g, 1.00 mmol) in 1,2-dichloroethane (35 mL) and CH_3CN (3 mL) was stirred for 20 min at room temperature. Ph_3SiCl (0.59 g, 2.00 mmol) was then added, and the mixture refluxed for 23 h. The solution was filtered at room temperature and treated with ethyl[3-(2-pyridyl)-1-pyrazolyl]acetate (0.25 g, 1.08 mmol). After stirring for 3 h at room temperature, the solution was evaporated to dryness, and the resultant solid product washed with diethyl ether (2 × 15 mL) and dried under reduced pressure (0.63 g, 69%). Anal. Calcd. for $C_{48}H_{43}N_3MoO_6Si_2$ (909.98): C, 63.35; H, 4.76; N, 4.62. Found: C, 63.62; H, 4.34; N, 4.81. IR (KBr): 3122w, 3065m, 3045w, 2996w, 1749vs, 1611m, 1589m, 1570w, 1508w, 1483m, 1439s, 1428vs, 1375m, 1261m, 1247m, 1214s, 1114vs, 1074m, 1027m, 999m, 927vs, 911sh, 900sh, 769s, 742s, 708vs,

700sh, 514vs, 504vs, 455w, 430w cm^{-1}. ^1H NMR (300.13 MHz, 25 °C, acetone-d_6): $\delta = 8.53$ ppm (d, 1H, H^{11}), 7.99 ppm (d, 1H, H^8), 7.90 ppm (dt, 1H, H^9), 7.73 ppm (d, 1H, H^5), 7.73–7.05 ppm (c, 31H, phenyl-H + H^{10}), 6.90 ppm (d, 1H, H^4), 5.01 ppm (s, 2H, N–CH_2), 4.06 ppm (q, 2H, O–CH_2), 1.12 ppm (t, 3H, CH_3).

2.4. *[$MoO_2(OSiPh_3)_2$[2-(1-butyl-3-pyrazolyl)pyridine]] (**4**)*

A suspension of Ag_2MoO_4 (0.70 g, 1.86 mmol) in 1,2-dichloroethane (35 mL) and CH_3CN (3 mL) was stirred for 20 min at room temperature. Ph_3SiCl (1.31 g, 4.44 mmol) was then added, and the mixture refluxed under nitrogen for 8 h. After cooling to room temperature, 2-(1-butyl-3-pyrazolyl)pyridine (0.38 g, 1.91 mmol) was added, and the mixture stirred at room temperature for 3 h. The solution was filtered, evaporated to dryness, and the resultant colourless solid washed with diethyl ether (2 × 15 mL), hexane (2 × 10 mL), and dried under reduced pressure (1.14 g, 70%). Anal. Calcd. for $C_{48}H_{45}N_3MoO_4Si_2$ (880.01): C: 65.51; H, 5.15; N, 4.77. Found: C, 65.05; H, 5.34; N, 4.98. IR (KBr): 1610m, 1439m, 1428s, 1370w, 1114s, 950sh, 931vs, 917sh, 901sh, 767w, 741m, 708vs, 702sh, 514s, 506sh, 457w, 429w cm^{-1}. ^1H NMR (300.13 MHz, 25 °C, acetone-d_6): $\delta = 8.63$ ppm (d, 1H, H^{11}), 8.10 ppm (d, 1H, H^8), 7.93 ppm (dt, 1H, H^9), 7.75 ppm (d, 1H, H^5), 7.68–7.10 ppm (c, 31H, phenyl-H + H^{10}), 6.93 ppm (d, 1H, H^4), 4.25 ppm (t, 2H, N–CH_2), 1.95–1.85 ppm (m, 2H, CH_2), 1.38–1.28 ppm (m, 2H, CH_2), 0.96 ppm (t, 3H, CH_3).

2.5. Crystal structure determination of *1*

Yellow crystals of [MoO_2Cl_2{ethyl[3-(2-pyridyl)-1-pyrazolyl]acetate}] (**1**) suitable for X-ray diffraction were prepared by slow diffusion of diethyl ether into a solution of **1** in CH_3CN. The structure was determined at 100 K using graphite monochromatised radiation. Data were collected on an APEX2 diffractometer [30]. Crystal data and experimental parameters are presented in Table 1. The data were corrected for Lorentz-polarisation effects and for absorption [31]. The structure was solved by direct methods using SIR97 [32] and refined by least-squares techniques using programs from the KRYSTAL package [33]. Hydrogen atoms were kept fixed in calculated positions with C–H = 0.95 Å and with isotropic displacement factors 20% larger than U_{eq} for the atoms to which they were bonded. Atomic scattering factors were taken from the International Tables for X-Ray Crystallography [34]. Crystallographic data for the structural analysis has been deposited with the Cambridge Crystallographic Data Centre, CCDC No. 607428. These data can be obtained free of charge at http://www.ccdc.cam.ac.uk/conts/retrieving.html [or from the Cambridge Crystallographic Data Centre, 12 Union Road, Cambridge CB2 1EZ, UK; Fax: (international) +44 1223 336 033; e-mail: deposit@ccdc.cam.ac.uk].

Table 1
Crystal data and structure refinement for [MoO_2Cl_2{ethyl[3-(2-pyridyl)-1-pyrazolyl]acetate}] (**1**)

Empirical formula	$C_{12}H_{13}Cl_2MoN_3O_4$
Formula weight	430.12
Crystal system	Tetragonal
Space group	$P4_1$ (no. 76)
a (Å)	8.3865(1)
b (Å)	8.3865(1)
c (Å)	22.7838(6)
V (Å^3)	1602.36(6)
Z	**4**
Reflections collected	113268
Independent (R_{int})	7743(0.076)
Observed ($I > 3\sigma I$)	4789
R indices ($I > 3\sigma I$) $R1$[a]	0.043
$wR1$	0.054
$\Delta\rho_{max}$, $\Delta\rho_{min}$(e Å^{-3})	1.6(3), −2.2(3)

[a] $R1 = \sum ||F_0| - |F_c|| / \sum |F_0|$,
$wR1 = (\sum ||F_0| - |F_c||)^2 / \sum w|F_0^2|^{1/2}$,
$w = 1/\{((\sigma F_0^2) + B + (1 + A)F_0^2)^{1/2} - |F_0|\}^2$, $A = 0.04$ and $B = 6.0$.

2.6. Ab initio calculations

Ab initio calculations were performed using the G03W program package [35] running on a personal computer. The fully optimised geometry, the harmonic vibrational wavenumbers and the infrared and Raman intensities were obtained at the B3LYP level, using the standard LanL2DZ basis set and effective core potentials. In order to provide the best fit with experimental values, the harmonic vibrational wavenumbers were scaled by a factor of 0.961 [36]. Due to the large size of the systems, the phenyl groups in complexes **3** and **4** were replaced by H atoms. Previous calculations have shown that the calculated wavenumbers around the Mo centre are not significantly affected by this approach [9]. The vibrational assignments were based on the atomic displacements and calculated intensities for complexes **1** and **2**.

2.7. Catalytic reactions with compounds *1–4* as catalysts

The liquid-phase catalytic epoxidations were carried out at 55 °C under air (atmospheric pressure) in a reaction vessel equipped with a magnetic stirrer and immersed in a thermostated oil bath. A 1% molar ratio of complex/substrate and a substrate/oxidant molar ratio of 0.65 (*t*-BuOOH, 5.5 M in decane) were used. The course of the reaction was monitored using a gas chromatograph (Varian 3800) equipped with a capillary column (SPB-5, 20 m × 0.25 mm) and a flame ionisation detector. The products were identified by gas chromatography–mass spectrometry (HP 5890 Series II GC; HP 5970 Series Mass Selective Detector) using He as carrier gas.

3. Results and discussion

3.1. Synthesis and characterisation of the dioxomolybdenum(VI) complexes

The bis(chloro) complexes **1** and **2** were obtained as microcrystalline powders by simple ligand exchange with the solvent adduct $MoO_2Cl_2(THF)_2$ at room temperature, while the triphenylsiloxy compounds **3** and **4** were prepared by the reaction of

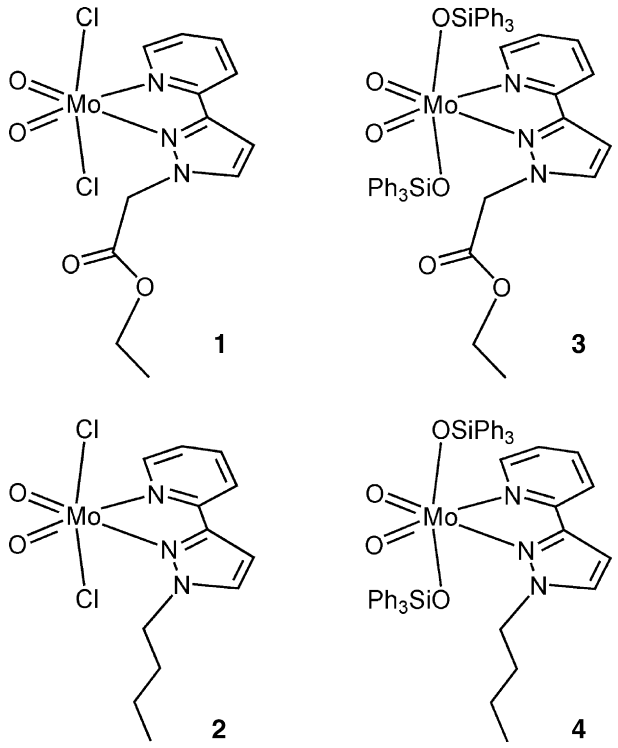

Plate 2.

silver molybdate with two equivalents of Ph_3SiCl and one equivalent of the respective pyrazolylpyridine (pzpy) ligand (Plate 2). Complexes **1**–**4** were characterised by elemental analysis, ^1H NMR, IR and Raman spectroscopy.

Table 2 lists the most characteristic and representative metal–ligand vibrations for the four complexes. Overall, there is a good qualitative agreement between experimental and calculated values, considering that the experimental spectra are for the condensed phase while the calculations consider only the isolated molecule. The symmetric and asymmetric Mo=O stretching modes of complexes **1** and **2** are observed as an intense doublet, which is typical for molybdenum complexes containing a *cis*-dioxo group [37]. For complexes **3** and **4**, the apparent absence of the symmetric and asymmetric Mo=O stretching bands in the IR spectra can be explained by their overlap with strong bands from the $MoO_2(OSiPh_3)_2$ fragment.

The vibrational modes of the equatorial MoO_2N_2 plane are easily discriminated in the vibrational spectra of **1**–**4**, as they were not influenced to a significant degree by the different natures of the Lewis base ligand. The weak Mo–N stretching modes are predicted from ab initio calculations to lie in different ranges for the bis(chloro) complexes (**1** and **2**) and the triphenylsiloxy complexes (**3** and **4**). As shown in Table 2, both the symmetric and asymmetric Mo–N stretching modes are observed in the Raman spectra, in the 120–170 cm^{-1} range for complexes **1** and **2**, and in the 190–290 cm^{-1} range for complexes **3** and **4**. An opposite trend is observed for the Mo=O stretching modes, which are found at lower frequencies in complexes **3** and **4**. These observations suggest that the strength of the interactions within the equatorial MoO_2N_2 plane changes from complexes **3** and **4** to **1** and **2**.

When comparing the Raman and IR spectra of complexes **1**–**4** with those of the corresponding free ligands and precursors, several changes ascribed to complex formation are observed, some of which are illustrated in Fig. 1 for complex **3**. The most significant differences, apart from the new bands at 900 and 912 cm^{-1} related to the Mo=O group, occur between 1550 and 1800 cm^{-1}. The bands arising from the C–N stretching ring vibrations, the C–C pyridine vibrations and the ligand N–C–C–N fragment reflect a general trend (also observed for the other complexes) to be shifted to higher wavenumbers upon coordination to the Mo centre. As shown in Fig. 1, the Raman bands of ethyl[3-(2-

Table 2
Representative Raman and IR stretching frequencies (cm^{-1}) of complexes **1**–**4** and calculated (B3LYP) frequencies

Assignment	**1**			**2**		
	Calculated[a]	IR[b]	Raman	Calculated[a]	IR	Raman
$\nu Mo{=}O_{sym}$	933	936s	937s	932	937s	935vs
$\nu Mo{=}O_{asym}$	912	900vs	901w	916	908vs	906m
$\nu Mo{-}Cl_{sym}$	278	–	215m	273	–	215m
$\nu Mo{-}Cl_{asym}$	309	343m	321sh	308	345m	–
$\nu Mo{-}N_{sym}$	149	–	170w	153	–	150w
$\nu Mo{-}N_{asym}$	159	–	123w	158	–	123w
Assignment	**3**			**4**		
	Calculated[a]	IR[b]	Raman	Calculated[a]	IR	Raman
$\nu Mo{=}O_{sym}$	949	911sh[c]	912vs	949	917sh[c]	916vs
$\nu Mo{=}O_{asym}$	901	900sh[c]	900s	901	901sh[c]	900s
$\nu Mo{-}O_{sym}$	376	430w	420vw	380	429w	422w
$\nu Mo{-}O_{asym}$	413	455w	–	411	457w	–
$\nu Mo{-}N_{sym}$	190	277m	284w	188	274m	275w
$\nu Mo{-}N_{asym}$	127	–	192w	132	–	191w

[a] Scaled values (scale factor = 0.961).
[b] sh: shoulder; vs: very strong; vw: very weak; m: medium; w: weak.
[c] Overlap with strong O–Si bands.

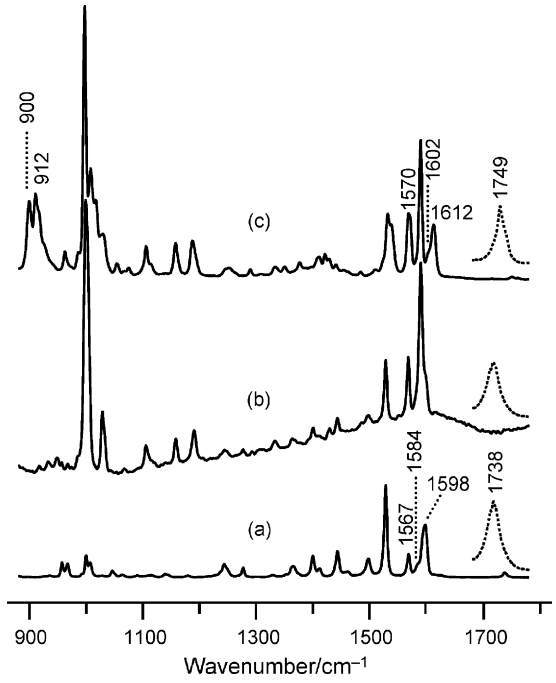

Fig. 1. Raman spectra (900–1800 cm^{-1} region) of ethyl[3-(2-pyridyl)-1-pyrazolyl]acetate (a), compared with the weighted sum of the spectra of the ligand and the four-coordinate compound $[MoO_2(OSiPh_3)_2]$ (b), and complex **3** (c). The insets (- - -) show the carbonyl stretching bands observed in the corresponding FT-IR spectra.

pyridyl)-1-pyrazolyl]acetate at 1567 cm^{-1} (pzpy C–C inter-ring stretching mode), 1584 cm^{-1} (py C–N stretching mode) and 1598 cm^{-1} (py C–C stretching mode) are shifted to 1570, 1602 and 1612 cm^{-1}, respectively, in complex **3**. Another effect of complexation involves the IR band assigned to the stretching of the carbonyl group, which shifts from 1738 cm^{-1} for ethyl[3-(2-pyridyl)-1-pyrazolyl]acetate to 1742 cm^{-1} for **1** and 1749 cm^{-1} for **3**. Since a weak C–H···O contact (263 ppm) between the pyrazolylpyridine ligands has been verified in the X-ray crystal structure of complex **1**, the shift of the carbonyl stretching band to higher frequencies in both complexes can be attributed to a weakening of C–H···O interactions upon coordination of the ligands to the molybdenum centres.

The crystal structure of complex **1** was determined by X-ray diffraction. This is the first reported structure for a dioxomolybdenum(VI) complex of the type $[MoO_2X_2L_2]$ bearing a bidentate pyrazolylpyridine ligand. Concerning the related oxodiperoxo molybdenum(VI) complexes $[MoO(O_2)_2L_2]$, there are several crystallographic investigations for species containing substituted pyrazolylpyridines [26,28,38,39]. Selected bond distances and angles for **1** are listed in Table 3. The compound is monomeric (Fig. 2). Molybdenum is coordinated to the nitrogen atoms of the pyrazolylpyridine group, Mo–N = 2.317(3) and 2.305(3) Å, two oxygen atoms with Mo–O = 1.697(3) and 1.704(3) Å, and two chlorine atoms with Mo–Cl = 2.392(1) and 2.343(1) Å. Both the pyrazolylpyridine moiety and the acetic acid ester group are planar and hinged at C9 which is common to both planes, the angle between the planes being 93.2°.

3.2. Catalytic tests

The catalytic performances of complexes **1**–**4** for epoxidation reactions were investigated using *cis*-cyclooctene as a model substrate and *t*-BuOOH as the oxygen donor. In a control experiment, carried out without catalyst, no reaction occurred, whereas in the presence of complexes **1**–**4** 1,2-epoxycyclooctane was obtained almost quantitatively within 7 h reaction, indicating that these compounds act as catalysts and exhibit excellent product selectivity. The initial catalytic epoxidation

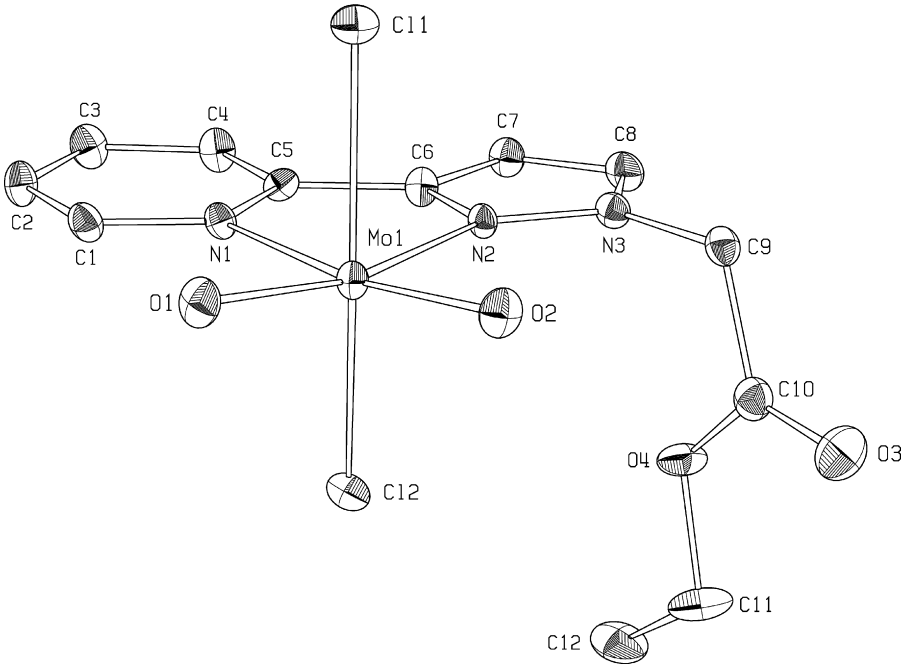

Fig. 2. Molecular structure of $[MoO_2Cl_2\{ethyl[3-(2-pyridyl)-1-pyrazolyl]acetate\}]$ (**1**).

Table 3
Selected bond distances (Å) and angles (°) for complex **1**

Mo1–N1	2.317(3)
Mo1–N2	2.305(3)
Mo1–O1	1.697(3)
Mo1–O2	1.704(3)
Mo1–Cl1	2.392(1)
Mo1–Cl2	2.343(1)
N1–Mo1–N2	69.7(1)
N1–Mo1–O1	90.3(1)
N1–Mo1–O2	163.4(1)
N1–Mo1–Cl1	80.57(8)
N1–Mo1–Cl2	81.76(8)
N2–Mo1–O1	159.7(1)
N2–Mo1–O2	93.7(1)
N2–Mo1–Cl1	79.88(8)
N2–Mo1–Cl2	82.88(8)
O1–Mo1–O2	106.1(1)
O1–Mo1–Cl1	93.5(1)
O1–Mo1–Cl2	98.4(1)
O2–Mo1–Cl1	95.6(1)
O2–Mo1–Cl2	98.0(1)
Cl1–Mo1–Cl2	158.68(3)

activities of the four complexes (160–347 mol mol_{Mo}^{-1} h^{-1}) are much greater than those found in the literature for several dioxomolybdenum(VI) complexes bearing Lewis base ligands, such as 2,2′-bipyridine (12–25 mol mol_{Mo}^{-1} h^{-1}) [9,17], ethylenediimine (63 mol mol_{Mo}^{-1} h^{-1}) [18] and 1,4-diazabutadiene (14–58 mol mol_{Mo}^{-1} h^{-1}) [40,41], as well as for the tricarbonyl complexes [(η^5-C_5H_5)Mo(CO)$_3$Cl], [(η^5-C_5H_4–COOMe)Mo(CO)$_3$Cl] and {[η^5-C_5H_4–CONH–C_3H_6-Si(OEt)$_3$]Mo(CO)$_3$Cl} (140, 40 and 13 mol mol_{Mo}^{-1} h^{-1}, respectively), which undergo oxidative decarbonylation in situ to give oxomolybdenum catalysts [42]. On the other hand, TOFs of 820 and 6000 h^{-1} were recently reported for the complex [(η^5-C_5H_5)Mo(CO)$_3$Me] with catalyst loadings of 1 and 0.1%, respectively [43].

In general, the mechanisms proposed for *t*-BuOOH-based epoxidation of olefins with Mo^{VI} complexes are heterolytic in nature, involving coordination of the oxidant to the metal centre, which acts as a Lewis acid thereby increasing the oxidising power of the peroxo group, and subsequently the olefin is epoxidised by nucleophilic attack on an electrophilic oxygen atom of the oxidising species [22]. Spectroscopic and computational methods applied to molybdenum dioxo and oxodiperoxo complexes bearing bipyridine and pyrazolylpyridine ligands, respectively, support a reaction mechanism involving an activation state formed between the complex, oxidant and olefin [17,25]. The by-product of the epoxidation reaction, *tert*-butanol, is a competitor to *t*-BuOOH for coordination to the metal centre, leading to the formation of inactive species and a consequent rapid decrease in the olefin conversion rate [17]. Similarly, for complexes **1**–**4**, the initial reaction rates are much higher than those observed later on in the reactions (Fig. 3).

Table 4
Catalytic performance of compounds **1**–**4** in cyclooctene epoxidation with *t*-BuOOH at 55 °C

Compound	Co-solvent	TOF (mol mol_{Mo}^{-1} h^{-1})[a]	Conversion (%)[b]	Selectivity (%)[b]
	None	328	93	100
1	1,2-Dichloroethane	109	80	100
	n-Hexane	12	22	100
2	None	347	92	100
	None	160	90	100
3	1,2-Dichloroethane	47	77	100
	n-Hexane	12	48	100
4	None	165	88	100

[a] Calculated at 10 min.
[b] Calculated at 4 h.

Table 5
Catalytic performance of complexes **1** and **3** in the epoxidation of olefins with *t*-BuOOH at 55 °C[a]

Olefin	**1**		**3**	
	Conversion (%)[b]	Selectivity (%)[c]	Conversion (%)	Selectivity (%)
Cyclooctene	100	100	100	100
1-Octene	25	100	34	100
Trans-2-octene	66	100	86	100
Cyclododecene	76	100	90	98[d]
Styrene	18	78[d]	45	54[d]
(*R*)-(+)-Limonene	95	100	100	100

[a] Typical reaction conditions during 24 h.
[b] Olefin conversion.
[c] Selectivity to the corresponding epoxide.
[d] The corresponding diol was formed.

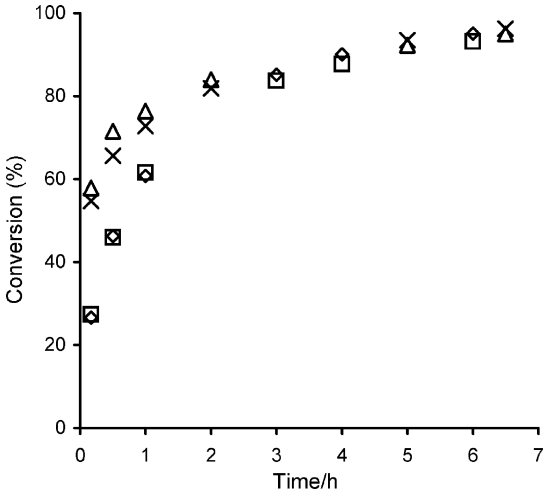

Fig. 3. Kinetics of the epoxidation of cyclooctene with *t*-BuOOH in decane at 55 °C, catalysed by compounds **1** (×), **2** (△), **3** (◇) and **4** (□).

The conversion versus time curves are practically coincident for the chloro complexes **1** and **2**, as well as for the triphenylsiloxy complexes **3** and **4**. In fact, the curves for all four complexes are coincident for reaction times longer than 2 h. For shorter reaction times, the chloro complexes are more active than the triphenylsiloxy complexes. Thus, the initial reaction rates for **1** and **2** are about double those found for **3** and **4** (Table 4). These results indicate that the substituent on the pyrazolyl N-atom does not have a major influence on catalytic activity, in contrast to the first sphere ligand (Cl or $OSiPh_3$). Considering the relative dimensions of the butyl and ethyl acetate groups, and their distances to the metal centre, one would not expect them to significantly alter the electronic and steric properties of the complex. Indeed, according to the Raman data, the strength of the interactions within the equatorial MoO_2N_2 plane seems to change mainly from complexes **3** and **4** to **1** and **2**. Furthermore, the compounds which differ only in the nature of the substituent on the pyrazolyl N-atom are roughly equally soluble in the reaction medium. The lower catalytic activity of **3** and **4** may be due to greater steric constraints and lower flexibility of the coordination geometry caused by the significantly bulkier $OSiPh_3$ axial ligands in comparison to Cl. The higher catalytic activities of **1** and **2** may also be due to their higher solubility in the reaction medium as compared with **3** and **4**.

The solvent effect was studied for complexes **1** and **3** using 1,2-dichloroethane or *n*-hexane, at 55 °C. No dependence of product selectivity on the solvent was observed. For both catalysts, initial activity and conversion at 4 h reaction follow the order: no co-solvent > 1,2-dichloroethane > *n*-hexane (Table 4). The negative effect of *n*-hexane and 1,2-dichloroethane on catalytic activity may be due to slight changes in the solubility of the catalyst. Comparable results have been reported for [$MoO_2(OSiPh_3)_2$(2,2′-bipyridine)], under similar reaction conditions [9].

The catalytic performance of **1** and **3** was investigated in the oxidation of other olefins, namely 1-octene, *trans*-2-octene, cyclododecene, (*R*)-(+)-limonene and styrene, at 55 °C. For both complexes the reaction is slower for terminal olefins,

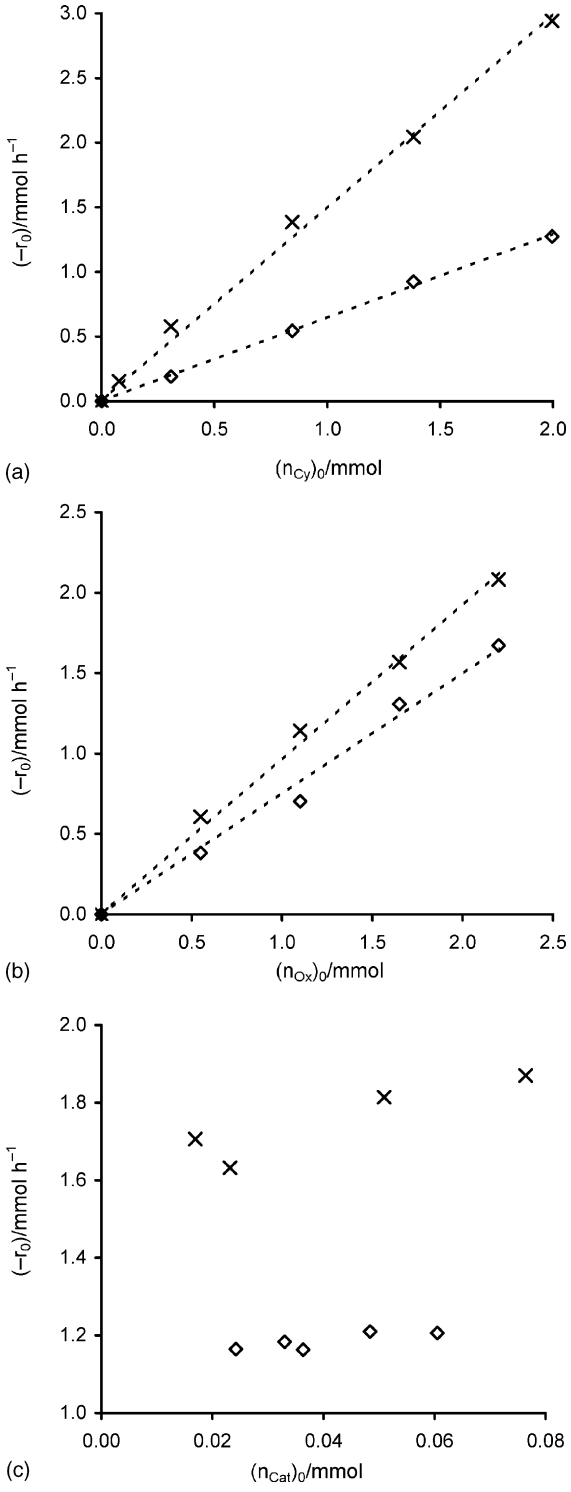

Fig. 4. Dependence of the initial reaction rate of cyclooctene epoxidation in the presence of compounds **1** (×) or **3** (◇) on initial amount of cyclooctene (a), *t*-BuOOH (b), and catalyst (c).

such as 1-octene and styrene, than for those bearing internal C=C bonds (Table 5). These results are consistent with the above mechanistic assumptions in that a lower activation barrier would be expected for the electrophilic attack on the more substituted olefins. Both compounds possess relatively high reactivity towards the epoxidation of *cis*-cyclooctene and (*R*)-

(+)-limonene. The compounds exhibit excellent regioselectivity (100% at >95% conversion) for the epoxidation of the endocyclic double bond of (*R*)-(+)-limonene. The slower reaction rate observed for cyclododecene in comparison to cyclooctene may result from steric effects that become more relevant for the bulkier olefin. For all olefins the corresponding epoxide was the only observed product, excluding cyclododecene and styrene, where the corresponding diol was also formed, most likely via consecutive epoxide ring opening.

The kinetics of the liquid-phase epoxidation of cyclooctene in the presence of **1** and **3** was further investigated using the method of initial rates ($-r_0$), keeping the total volume of the reaction mixture constant using decane (the solvent of the purchased *t*-BuOOH) as solvent. The dependence of the initial rate of cyclooctene conversion ($-r_0$) on either the initial amount of cyclooctene $(n_{Cy})_0$ or the initial amount of oxidant $(n_{Ox})_0$ was studied for initial concentrations of cyclooctene or oxidant $\leq 1.5\,mol\,dm^{-3}$, at 55 °C. Under the applied operating conditions, the reaction does not take place in the absence of *t*-BuOOH. For both complexes **1** and **3**, the plots of ($-r_0$) against $(n_{Cy})_0$ or $(n_{Ox})_0$ are linear ($R^2 = 0.99$), suggesting apparent first order dependences with respect to cyclooctene or oxidant concentration (Fig. 4).

The dependence of ($-r_0$) on the initial amount of catalyst $(n_{Cat})_0$ was studied in the range of 17–80 μmol (1.7 mmol olefin), at 55 °C (Fig. 4c). For complexes **1** and **3** ($-r_0$) is practically independent of $(n_{Cat})_0$, suggesting an apparent zero order dependence. Within the studied range of catalyst quantities, complexes **1** and **3** were not completely soluble and increasing the amount of catalyst led to more precipitate in the reaction medium. Due to the negligible specific surface areas of **1** and **3**, these compounds are essentially catalytically inactive in heterogeneous phase. Hence, the active species responsible for cyclooctene conversion are the soluble fractions of compounds **1** and **3**, and increasing the catalyst amount above the saturation point of the catalyst solution (under the applied reaction conditions) does not have any major effect on olefin conversion.

4. Conclusion

The present work has reinforced previous findings that the variation of the first-sphere ligands in distorted octahedral complexes of the type $[MoO_2X_2L_2]$ can lead to excellent catalysts for olefin epoxidation. Indeed, for cyclooctene epoxidation by *t*-BuOOH at 55 °C, the turnover frequencies for complexes bearing substituted pyrazolylpyridine ligands are approximately one order of magnitude greater than those for the corresponding complexes bearing ligands derived from 2,2′-bipyridine. The pyrazolylpyridine ligand system has the additional advantage that long alkyl side chains can be easily introduced, leading to excellent solubility of the derived molybdenum catalysts in organic solvents. A variation of the donor strength of these ligands should also be possible by the inclusion of electron donating or withdrawing groups attached to the heteroaromatic rings. We are continuing our efforts along these lines to obtain even more effective oxomolybdenum catalysts with tailored properties.

Acknowledgments

The authors are grateful to FCT, OE and FEDER for funding (Project POCI/CTM/58507/2004). SMB thanks the University of Aveiro for a research grant. MN, CCLP and MSB are grateful to the FCT for PhD and post-doctoral grants.

References

[1] G.-S. Kim, D. Huffman, C.W. DeKock, Inorg. Chem. 28 (1989) 1279.
[2] M.H. Chisholm, K. Folting, J.C. Huffman, C.C. Kirkpatrick, Inorg. Chem. 23 (1984) 1021.
[3] T.A. Hanna, C.D. Incarvito, A.L. Rheingold, Inorg. Chem. 39 (2000) 630.
[4] M. Weidenbruch, C. Pierrard, H.Z. Pesel, Naturforschung 33B (1978) 1468.
[5] J. Jarupatrakorn, M.P. Coles, T.D. Tilley, Chem. Mater. 17 (2005) 1818.
[6] M. Huang, C.W. DeKock, Inorg. Chem. 32 (1993) 2287.
[7] F.E. Kühn, A.M. Santos, M. Abrantes, Chem. Rev. 106 (2006) 2455.
[8] A. Thapper, J.P. Donahue, K.B. Musgrave, M.W. Willer, E. Nordlander, B. Hedman, K.O. Hodgson, R.H. Holm, Inorg. Chem. 38 (1999) 4104.
[9] S.M. Bruno, B. Monteiro, M.S. Balula, C. Lourenço, A.A. Valente, M. Pillinger, P. Ribeiro-Claro, I.S. Gonçalves, Molecules 11 (2006) 298.
[10] F.E. Kühn, E. Herdtweck, J.J. Haider, W.A. Herrmann, I.S. Gonçalves, A.D. Lopes, C.C. Romão, J. Organomet. Chem. 583 (1999) 3.
[11] F.J. Arnáiz, R. Aguado, M.R. Pedrosa, A. De Cian, Inorg. Chim. Acta 347 (2003) 33.
[12] N. Manwani, M.C. Gupta, R. Ratnani, J.E. Drake, M.B. Hursthouse, M.E. Light, Inorg. Chim. Acta 357 (2004) 939.
[13] M.B. Hursthouse, W. Levason, R. Ratnani, G. Reid, Polyhedron 23 (2004) 1915.
[14] G. Wang, G. Chen, R.L. Luck, Z. Wang, Z. Mu, D.G. Evans, X. Duan, Inorg. Chim. Acta 357 (2004) 3223.
[15] M.D. Brown, M.B. Hursthouse, W. Levason, R. Ratnani, G. Reid, Dalton Trans. (2004) 2487.
[16] F.E. Kühn, A.D. Lopes, A.M. Santos, E. Herdtweck, J.J. Haider, C.C. Romão, A.G. Santos, J. Mol. Catal. A: Chem. 151 (2000) 147.
[17] F.E. Kühn, M. Groarke, É. Bencze, E. Herdtweck, A. Prazeres, A.M. Santos, M.J. Calhorda, C.C. Romão, I.S. Gonçalves, A.D. Lopes, M. Pillinger, Chem. Eur. J. 8 (2002) 2370.
[18] Ž. Petrovski, M. Pillinger, A.A. Valente, I.S. Gonçalves, A. Hazell, C.C. Romão, J. Mol. Catal. A: Chem. 227 (2005) 67.
[19] L.R. Florian, E.R. Corey, Inorg. Chem. 7 (1968) 722.
[20] D.C. Brewer, J.L. Templeton, D.M.P. Mingos, J. Am. Chem. Soc. 109 (1987) 5203.
[21] G. Barea, A. Lledos, F. Maseras, Y. Jean, Inorg. Chem. 37 (1998) 3321.
[22] C.D. Nunes, A.A. Valente, M. Pillinger, J. Rocha, I.S. Gonçalves, Chem. Eur. J. 9 (2003) 4380.
[23] A.A. Valente, J. Moreira, A.D. Lopes, M. Pillinger, C.D. Nunes, C.C. Romão, F.E. Kühn, I.S. Gonçalves, New J. Chem. 28 (2004) 308.
[24] S.M. Bruno, J.A. Fernandes, L.S. Martins, I.S. Gonçalves, M. Pillinger, P. Ribeiro-Claro, J. Rocha, A.A. Valente, Catal. Today 114 (2006) 263.
[25] W.R. Thiel, J. Eppinger, Chem. Eur. J. 3 (1997) 696.
[26] W.R. Thiel, M. Angstl, T. Priermeier, Chem. Ber. 127 (1994) 2373.
[27] W.R. Thiel, M. Angstl, N. Hansen, J. Mol. Catal. A: Chem. 103 (1995) 5.
[28] W.R. Thiel, T. Priermeier, Angew. Chem. Int. Ed. Engl. 34 (1995) 1737.
[29] W.M. Carmichael, D.A. Edwards, G.W.A. Fowles, P.R. Marshall, Inorg. Chim. Acta 1 (1964) 93.
[30] Bruker-Nonius, APEX2, Version 1.8–6, Bruker-Nonius BV, Delft, The Netherlands, 2003.
[31] Siemens SMART, SAINT and XPREP Area-Detector Control and Integration Software, Siemens Analytical X-Ray Institute Inc., Madison, WI, USA, 1995.

[32] A. Altomare, G. Cascareno, G. Giacovazzo, A. Guagliardi, A.G.G. Moliterni, M.C. Burla, G. Polidori, M. Camalli, R. Spagna, SIR97, University of Bari, Italy, 1997.
[33] A. Hazell, KRYSTAL: An Integrated System of Crystallographic Programs, Aarhus University, Denmark, 1995.
[34] International Tables for X-Ray Crystallography, vol. IV, Kynoch Press, Birmingham, 1974 (present distributor: Kluwer, Dordrecht).
[35] M.J. Frisch, G.W. Trucks, H.B. Schlegel, G.E. Scuseria, M.A. Robb, J.R. Cheeseman, J.A. Montgomery Jr., T. Vreven, K.N. Kudin, J.C. Burant, J.M. Millam, S.S. Iyengar, J. Tomasi, V. Barone, B. Mennucci, M. Cossi, G. Scalmani, N. Rega, G.A. Petersson, H. Nakatsuji, M. Hada, M. Ehara, K. Toyota, R. Fukuda, J. Hasegawa, M. Ishida, T. Nakajima, Y. Honda, O. Kitao, H. Nakai, M. Klene, X. Li, J.E. Knox, H.P. Hratchian, J.B. Cross, C. Adamo, J. Jaramillo, R. Gomperts, R.E. Stratmann, O. Yazyev, A.J. Austin, R. Cammi, C. Pomelli, J.W. Ochterski, P.Y. Ayala, K. Morokuma, G.A. Voth, P. Salvador, J.J. Dannenberg, V.G. Zakrzewski, S. Dapprich, A.D. Daniels, M.C. Strain, O. Farkas, D.K. Malick, A.D. Rabuck, K. Raghavachari, J.B. Foresman, J.V. Ortiz, Q. Cui, A.G. Baboul, S. Clifford, J. Cioslowski, B.B. Stefanov, G. Liu, A. Liashenko, P. Piskorz, I. Komaromi, R.L. Martin, D.J. Fox, T. Keith, M.A. Al-Laham, C.Y. Peng, A. Nanayakkara, M. Challacombe, P.M.W. Gill, B. Johnson, W. Chen, M.W. Wong, C. Gonzalez, J.A. Pople, GAUSSIAN 03. Revision B.04, Gaussian Inc., Pittsburgh, PA, 2003.
[36] R.D. Johnson III (Ed.), NIST Computational Chemistry Comparison and Benchmark Database, NIST Standard Reference Database Number 101, Release 12, 2005, http://srdata.nist.gov/cccbdb.
[37] K. Nakamoto, Infrared and Raman Spectra of Inorganic and Coordination Compounds, John Wiley, 1997.
[38] H. Glas, M. Spiegler, W.R. Thiel, Eur. J. Inorg. Chem. (1998) 275.
[39] M.J. Hinner, M. Grosche, E. Herdtweck, W.R. Thiel, Z. Anorg. Allg. Chem. 629 (2003) 2251.
[40] C.D. Nunes, M. Pillinger, A.A. Valente, A.D. Lopes, I.S. Gonçalves, Inorg. Chem. Commun. 6 (2003) 1228.
[41] C.D. Nunes, M. Pillinger, A.A. Valente, J. Rocha, A.D. Lopes, I.S. Gonçalves, Eur. J. Inorg. Chem. (2003) 3870.
[42] M. Abrantes, S. Gago, A.A. Valente, M. Pillinger, I.S. Gonçalves, T.M. Santos, J. Rocha, C.C. Romão, Eur. J. Inorg. Chem. (2004) 4914.
[43] J. Zhao, A.M. Santos, E. Herdtweck, F.E. Kühn, J. Mol. Catal. A: Chem. 222 (2004) 265.